Fluorescent unsymmetrical four-ring bent-core mesogens: 2D modulated phases

Article *in* CrystEngComm · December 2013

DOI: 10.1039/c3ce41360h

CrystEngComm

RSC Publishing

PAPER

View Article Online
View Journal | View Issue

Cite this: *CrystEngComm*, 2013, **15**, 10510

Fluorescent unsymmetrical four-ring bent-core mesogens: 2D modulated phases†

Rahul Deb,[a] Atiqur Rahman Laskar,[a] Dipika Debnath Sarkar,[a] Golam Mohiuddin,[a] Nirmalangshu Chakraborty,[a] Sharmistha Ghosh,[b] D. S. Shankar Rao[c] and Nandiraju V. S. Rao*[a]

Received 11th July 2013,
Accepted 3rd October 2013

DOI: 10.1039/c3ce41360h

www.rsc.org/crystengcomm

Based on the chemical incompatibility between the aromatic mesogenic cores and the flexible end aliphatic (methylene units) chains, which can lead to the formation of polarization modulated layered undulated phases, four-ring bent-core compounds have been designed and synthesized. The designed compounds are thermally and hydrolytically stable due to intramolecular hydrogen bonding, highly fluorescent and exhibit 2D-polarization modulated layer undulated (PMLU) smectic phases. The phase transition temperatures have been confirmed by differential scanning calorimetry and the phases are confirmed by polarizing optical microscopy and X-ray diffraction studies. For compounds **1-10-11** and **1-15-11** the peaks are indexed to tilted columnar lattice (Col_{ob}), while for **2-12-11** the peaks are indexed to the rectangular lattice belonging to the PMLU family The influence of the direction of ester linking group played an important role in the mesophase as well as the evaluated parameters of the dipole moment, the bending angle and the asymmetry parameter by spin-restricted DFT calculations using the B3LYP exchange-correlation functional and the 6-311G(d,p) basis set.

1. Introduction

The discovery of polar and chiral order in the bent-core compounds[1,2] promoted the importance of the bent or banana or V-shaped liquid crystals (BLC) as a new sub-field of liquid crystals. Because of the sterically induced packing of these bent-core molecules several new smectic modifications,[3–9] in addition to lamellar structures with one-dimensional density modulation (B2 phases), can be realized which have no counterpart in the field of calamitic liquid crystals. On the other hand, molecular structural modifications of these new mesophases can lead to unusual physical properties which are not only interesting from the theoretical point of view but also in practical applications. Some of the unusual properties include chiral phases (nematic, B2, B4, B7 *etc.*) from achiral molecular assemblies with segregation into domains of opposite handedness,[10] and the formation of cybotactic clusters[11] in nematic phases *etc.* The much needed characteristic property for the polar order of smectic C phase, possessing the dual properties *viz.*, molecular chirality and director tilt (together responsible for polar order), is generated from chiral molecular assembly because chirality breaks inversion symmetry.[12] However based on symmetry considerations the ferroelectricity, ascribed to the polar C_{2v} symmetry, can be obtained from the efficient packing of bent-core (banana-shaped or bow-shaped or V-shaped) molecules into layers. In these bent-core molecules exhibiting the homogeneous layered banana phases, unique polar[1,4,5] and chiral[2,4,5] characteristic properties are realized due to their anisotropic molecular shapes and distinct tilt ordering of the packed bent-core molecules present in the layers. In such layered structures the antiparallel arrangement of molecular dipoles in adjacent layers compensates spontaneous electric polarization. Theoretically the bent molecular shape of π-bridged systems with electron push–pull moieties exhibiting polar order and mesomorphism[13] is appropriate for the correct design of non-linear optical materials. The use of topographic patterning by the confinement of helical nano filaments (HNFs) to control effects such as shear flow and temperature gradients may prove to be a powerful combination for possible applications in organic electronics.[14] Similarly uniformly aligned HNF materials over millimetre range are intriguing in functional material science.[15] As a consequence of the special molecular packing of these bent molecules, smectic layers with C_{2v}, C_2 and also C_{1h} or C_1 symmetry are realized[16] giving rise to ferro-, ferri- or antiferro-electric properties. Schematic representations of two important layered phases (of monoclinic C_2 symmetry and triclinic C_1 symmetry) have been outlined in Fig. 1. The chemical incompatibility

[a] *Chemistry Department, Assam University, Silchar 788011, India. E-mail: nandirajuv@gmail.com; Fax: +91 3842 270802; Tel: +91 3842 270943*
[b] *Department of Spectroscopy, Indian Association for the Cultivation of Science, Kolkata 700032, India*
[c] *Centre for Soft Matter Research, Jalahalli, Bangalore 560013, India*

† Electronic supplementary information (ESI) available. See DOI: 10.1039/c3ce41360h

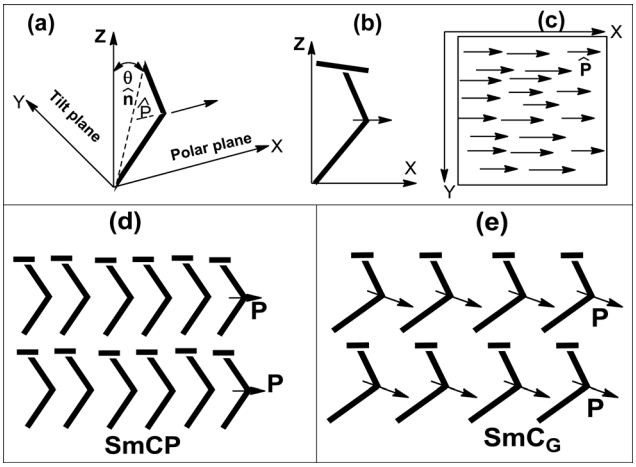

Fig. 1 (a) Possible single tilted bent-core molecular structure in the layered phase. In-plane polar order of the layer polarization in fluid phase. (*XY*, layer plane, *XZ* polar plane, and *YZ* tilt plane). (b) The tilt of the molecule is indicated by the bar at the end of the molecule, which is closer to the observer. (c) Top view of the polar order in the XY plane. Two dimensional and three dimensional molecular arrangements. Two important polar smectic structures formed by bent-shape molecules. Vectors indicate the layer polarizations. (d) In the SmCP structure (monoclinic C_2 symmetry), the long axis and the molecular plane tilt ("clinic") with respect to the layer normal. (e) The SmC_G (SmCTP) phase (triclinic C_1 symmetry) has a double tilted structure (G stands for general), *i.e.*, the molecular plane and the long axis are tilted in different directions (T stands for the tilt along the molecular plane).

between the aromatic mesogenic cores and the flexible end aliphatic (methylene units) chains leads to micro-segregation. Such micro-segregation has been supported by the presence of the molten state of alkyl chains in liquid crystalline (LC) states *viz.*, cubic LC phase,[17] SmE phase[18] (which is the closest to an ordered crystal) as well as the induction of the SmA phase[19] in binary cyanobiphenyl-*n*-heptane systems. In calamitic liquid crystals such incompatible units lead to the formation of one dimensional (1-D) uniform smectic layers of mesogenic aromatic cores and aliphatic regions and with the interlayer boundary regions prominently occupied by the alkyl chains. Furthermore, in mesomorphic rod like molecules possessing strong polar terminal moieties[20] and in polycatenar compounds,[21] columnar 2D modulated phases made of broken layers are well known. However in some BLCs multiple peaks in the x-ray scattering in the small angle region indicated additional order due to layer undulations (ripples)[22,23] beyond the one-dimensional stack of smectic layers. In these BLCs, decoupling between the polarization and tilt order makes the homogeneous layered structure unstable allowing linear polarization splay term in free energy density followed by nucleation of defects favoured by the polarization splay term. The splay is due to two factors a) steric contribution due to the efficient packing of the rigid cores and b) entropic contribution due to fluctuating end aliphatic chains. The mismatch or incompatibility between the cross sections of the aromatic core and aliphatic chain regions of the bent-core molecules[9,23*f*] in the bulk can possibly lead to spontaneous curvature with spatial modulation of the layers. One possible escape from the unequal surface area imbalance[23*h*] (local layer dilation) is the buckling of layers and the formation of sinusoidal or triangular-type phases which can be described as columnar structures of layer fragments. Hence to restore the system stability the uniform 1-D layers can break and transform into 2-D density modulated systems due to the splay of the molecular dipole organization to compensate macroscopic polarization.

In particular, bent-core systems possessing polar organization tend to form spontaneously polar and chiral layers leading to the B_2 phase with four possible local layer structures depending upon the relative polarity and chirality of adjacent layers. Additionally closely related phases with a myriad of 2-D modulated structures[22–24] due to the manifestation of an energetically favourable polarization splay are also reported. Prominent among them are the B_7 and B_1 phases and the schematic representations are shown in Fig. 2. The B_7 phase possesses a structure of continuous periodically undulated smectic layers[22] resulting from the local polarization splay. However the B_1 related phases consist of a structure of blocks of smectic layering organized into two-dimensional (2D) columnar[22,23] like lattices which is also understood on the basis of polarization splay. Most importantly the majority of these modifications are confined to five, six and seven ring systems with different central cores, linking groups, substituents, end alkyl(oxy) or siloxane moieties to name a few. In the empirical observations to realise molecules that exhibit mesophases characteristic of bent-core materials, five rings are required. Studies on the influence of the core structure in the formation of modulated phases revealed[23*m*] that an

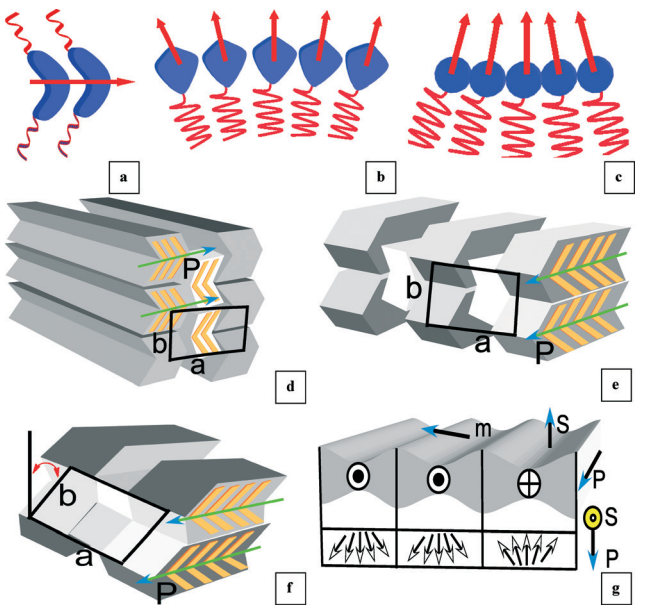

Fig. 2 (a) The schematic representations of aligned bent-core molecules. The arrow represents the dipole-moment. (b) The splay possibility due to the central rigid core efficient packing of molecules, (c) the splay possibility due to flexible end chain fluctuations. The splay polarization modulated and layer undulated structures, the layer structure of the molecules in the (d) B_1 phase (e) B_{1Rev} and (f) $B_{1Revtilt}$ (g) of B_7 phase. The arrows indicate the *P* vector (polarization) in the column, "*a* and *b*" are the dimensions of the crystallographic unit cell. S abbreviates splay and m abbreviates modulation.

increase in the size of core structure (rings 5 to 7) has to be compensated by an increase in the chain length to realize columnar structures. There are now thousands of bent-core molecules reported,[3–5] but only a few systems of four ring bent-core mesogens. Hence the possible changes, in the design of the molecular structure that can lead to an unsymmetrical molecular structure, are a reduction in the number of phenyl rings in one of the wings, with unequal and long alkyl chain lengths. The other possible change is the introduction of two different functionalities like amino and carboxylic groups or hydroxyl and carboxylic groups with or without a substituent at the bay position in the central phenyl ring followed by its extension to yield unsymmetrical molecules. The four-ring achiral unsymmetrical compounds are at the boundary between banana shaped and rod-like liquid crystals.[25]

In spite of the initial attempts to realize the banana mesomorphism in four-ring compounds not being encouraging,[25] the proper design with pro-mesomorphic linking groups and the synthesis of four-ring bent-core systems exhibiting banana mesomorphism[26] has been successfully demonstrated recently. The designed bent-core unsymmetrical molecule possesses four phenyl rings with three in one wing including the central ring and one ring in the other wing joined through imine–ester–imine linkages to make it an unsymmetrical molecule to exhibit polarization modulated layer undulated smectic phases. The reduction in the number of aromatic rings aided by unequal chain lengths in the two wings can modify the packing constraints of five ring BLCs. As a consequence of the lesser rigidity and a change in the packing mode one can expect lower transition temperatures and different mesomorphic properties in comparison to five or six ring systems. Furthermore, the imine linkage is stabilised by the ortho-hydroxyl group through H-bonding. One of the end alkoxy groups is fixed and the other end was varied. The modification of the angular 3,4'-disubstituted biphenyl central unit with the introduction of an ester linkage and its reversal between the two phenyl rings led to two novel polar central cores with structural variation for the possible extension of the bent-core molecular architecture. The ester linkage with benzene (1,3-substituted) or naphthalene (2,7-substituted) as the central core in BLCs has been established for its stability and resistance to degradation. It has been demonstrated earlier that the direction of the ester linkage[27] shows a strong influence on the mesophase behaviour and the physical properties in bent-core compounds. The nonplanarity in the central phenyl benzoate core, which is due to the ester linkage with a dihedral angle of 50–70°, between the phenyl carbon and the oxygen atom of the ester linkage,[28] can influence and lower the mesomorphic-isotropic clearing temperatures with a greater effect than the other linking groups. Furthermore, the longer terminal end alkyl chains govern the interlayer molecular order and hence the interlayer steric interactions play an important role to realize a variety of phase structures.[29] The electrostatic or steric interactions between the neighbouring molecules due to the special shape[30] of the bent-core molecules not only lead to spontaneous layer bending and polarization splay modulations but also a reduction from C_2 to C_1 symmetry of 2D modulated phases. To examine the influence of the direction of the ester linkage on the phase behaviour, the transition temperatures and the phase structure of these four ring systems, few homologues have been synthesized and their properties have been characterized by different techniques. Unlike the bent mesogenic dimers the reported compounds represent a novel class of bent shaped molecules comprised of four phenyl rings. In this paper we describe the synthesis and characterization of these materials in order to study the effect of the terminal chain length and in turn the importance of the interlayer interaction in bent-core liquid crystals containing four aromatic rings with ester and imine linkages as well as the direction of the ester linkage.

2. Experimental

All the chemicals were procured from M/s Alfa Aesar, Aldrich or Tokyo Kasei Kogyo Co. Ltd. The solvents and reagents are of AR grade and were distilled and dried before use. A micro analysis of the C and H elements was determined on a Perkin-Elmer 2400 elemental analyzer. IR spectra were recorded on a Shimadzu IR Prestige-21, FTIR-8400S (ν_{max} in cm^{-1}) on KBr disks. The ^1H nuclear magnetic resonance spectra were recorded on a Bruker DPX-400 spectrometer in a $CDCl_3$ (chemical shift δ in parts per million) solution with TMS as the internal standard. The UV–visible absorption spectra of the compounds in $CHCl_3$ at different concentrations were recorded on a Shimadzu UV-1601PC spectrophotometer (λ_{max} in nm). The fluorescence spectra of the compounds in chloroform were recorded with a Shimadzu RF-5301PC Spectroflouorometer with a 150 W xenon lamp as the excitation source. The liquid crystalline properties of the compounds were characterized using a polarizing microscope (Nikon optiphot-2-pol attached with hot and cold stage HCS302, with STC200 temperature controller configured for HCS302 from INSTEC Inc. USA). The phase transition temperatures and associated enthalpies were recorded using differential scanning calorimetry (Perkin-Elmer Pyris-1 system) with a heating/cooling rate of 5 °C min^{-1}. The details of the X-ray diffraction (XRD) studies have been reported earlier.[31] The apparatus essentially involves a high-resolution X-ray powder diffractometer (PANalytical X'Pert PRO) equipped with a high-resolution fast detector PIXCEL.

3. Results and discussion

[4-(*N*-4'-alkyloxysalicylidenemino)benzoate]-[3-(*N*-4'-alkyloxysalicylideneamino) phenyl] [1-*n*-*m*] and [3-(*N*-4'-alkyloxysalicylideneamino)benzoate]-[4-(*N*-4'-alkyloxysalicylidene-amino) phenyl]: (2-*n*-*m*)

The important requirement for achieving polar order and chirality in any of the materials is that the individual constituent molecule should possess a bent shape in the central core, and the non-coplanarity of the phenyl rings in the molecule

results in a noncentrosymmetric and non-coplanar architecture. In attempting to devise a strategy for the synthesis of bent-shaped molecules, the phenyl rings in the angular 3,4' and 4,3'-disubstituted biphenyl central unit[26] are separated by an ester linkage to yield two different central cores 3-aminophenyl-4-aminobenzoate and 4-aminophenyl-3-aminobenzoate. These model central moieties, which can be extended on both sides, possess sufficient bent shapes and are unsymmetrical in nature, which yields unsymmetrical molecules with the required perturbation in the form of a shape factor and changes in the dipole moment direction. However the two parts of the unsymmetrical bent-core molecule were derived from the reaction between 4-*n*-alkoxysalicylaldehyde with 3-aminophenol or 4-aminobenzoic acid. The synthesis of individual segments can lead to desired unsymmetrical end alkyl chain lengths. A further esterification reaction between the phenol and acid moieties yielded the proposed compounds. The synthesis of the designed compounds **1-*n*-*m*** (***m*** = 11, ***n*** = 10, 12, 13, 14, 15 and 16; ***m*** = 15, ***n*** = 11) and **2-*n*-*m*** (***m*** = 11, ***n*** = 10, 12, 14 and 16; ***m*** = 12, 13 and 15, ***n*** = 11) are presented in Scheme 1 and the details of the representative compounds are presented in the ESI.† The chemical structures of the final compounds are confirmed by the elemental analysis and spectral techniques (^{1}HNMR and FTIR spectroscopy) and the data of the representative compounds are presented in the ESI.† The analytical data is in good agreement with their chemical structures.

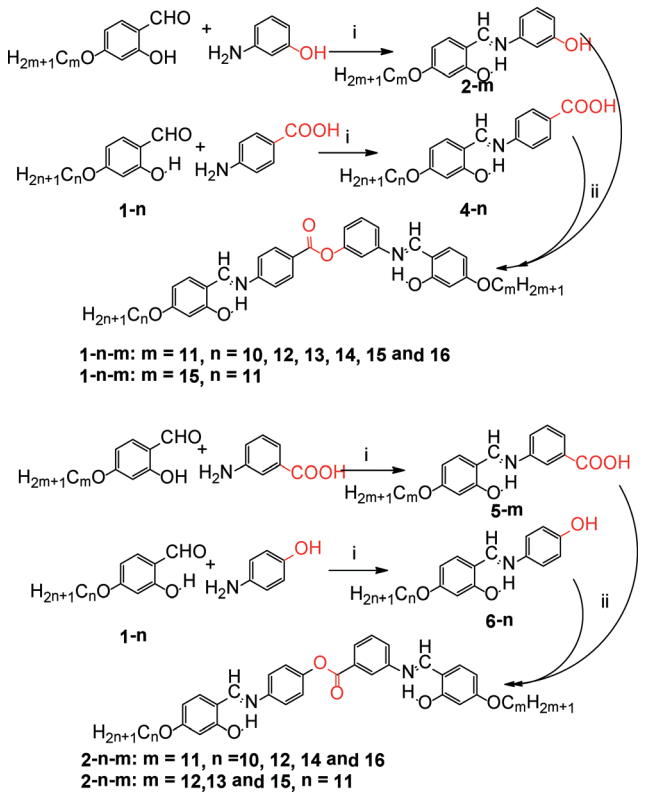

Scheme 1 Reagents and conditions. (i) Ethanol, a few drops of glacial AcOH, Δ 4 h; (ii) DCC, DMAP, DCM, 48 h.

Mesomorphic properties: polarizing optical microscopy (POM) and differential scanning calorimetry (DSC) studies

The four ring molecule possesses two OH groups in both the wings and through intramolecular H-bonding stabilize the imine linkages of the molecule. The modification of the angular 3,4'-disubstituted biphenyl unit with the introduction of an ester linkage *viz*., COO or OOC moiety between the two phenyl units leads to structural variation of the polar groups in the bent-core molecules and hence can promote a broad range of interesting variations in their mesogenic properties. Any variation in the length of the end alkyl chains changes the molecular interactions. As a part of our work on four-ring bent-core systems we modified the central core design with opposite directions of carbonyl moiety of the ester linkage. Both the wings are unsymmetrical and unequal in length and deviate significantly from the typical symmetrical and/or V-shape of other bent-core molecules.

The transition temperatures, enthalpies and entropies associated with the phase transitions of all of the compounds of the homologous series **1-*n*-*m*** (***m*** = 11, ***n*** = 10, 12, 13, 14, 15 and 16; ***m*** = 15, ***n*** = 11) and **2-*n*-*m*** (***m*** = 11, ***n*** = 10, 12, 14 and 16; ***m*** = 12, 13 and 15, ***n*** = 11) obtained from DSC at a scan rate of 5 °C min^{-1} in the second heating and cooling scans are presented in Table 1. The DSC spectra of two representative compounds **1-11-15** and **2-12-11** are presented in Fig. S1.† All of the compounds exhibit an enantiotropic mesomorphic behaviour except for **2-10-11**. The molecule is made up of two parts with one wing shorter than the other wing. The shorter wing is fixed with 4-*n*-undecyloxy salicylaldimine, while the length of the *n*-alkyloxy chain is varied in the longer wing of the molecule. All of the compounds were found to exhibit one mesophase only, exhibiting similar textures. **2-10-11** exhibits a monotropic LC phase. The mesomorphic properties of the materials in series 1 and series 2 which differ in the orientation of the ester linkage are found to differ in their transition temperatures as well as their mesomorphic range. The high stabilities of the compounds were demonstrated by the absence of any significant perturbation of the DSC patterns following several heating–cooling cycles (Fig. S2 and S3 (ESI†)).

Upon the very slow cooling of a thin film of the isotropic liquid of different homologues of the homologous series **1-*n*-*m*** different types of textures were observed as displayed in Fig. 3a–h, which are characteristic of 2D modulated layer undulated smectic phases (B7/B1$_{\mathrm{RevTilt}}$ phases). The common textures observed are the spiral domains of the telephone-wire structures resembling the B7 phase (Fig. 3a–c) on very slow cooling, the pseudo broken focal conic-fan or circular domains texture with dark extinction crosses (Fig. 3d) coinciding with the direction of the polarizer and analyser and long leaf like textures. Some representative optical textures of the compounds **1-12-11** in a polyimide coated ITO cell and

Table 1 The phase transition temperatures (°C) and mesomorphic thermal range of compounds **1-*n*-*m*** (***m*** = 11, ***n*** = 10, 12, 13, 14, 15 and 16; ***m*** = 15, ***n*** = 11) and **2-*n*-*m*** (***m*** = 11, ***n*** = 10, 12, 14 and 16; ***m*** = 12, 13 and 15, ***n*** = 11), recorded for second heating (first row) and second cooling (second row) cycles at 5 °C min^{-1} from DSC and confirmed by polarized optical microscopy. The enthalpies (ΔH in kJ mol^{-1}) and entropies (ΔS in J mol^{-1} K^{-1}) respectively are presented in the parentheses[a]

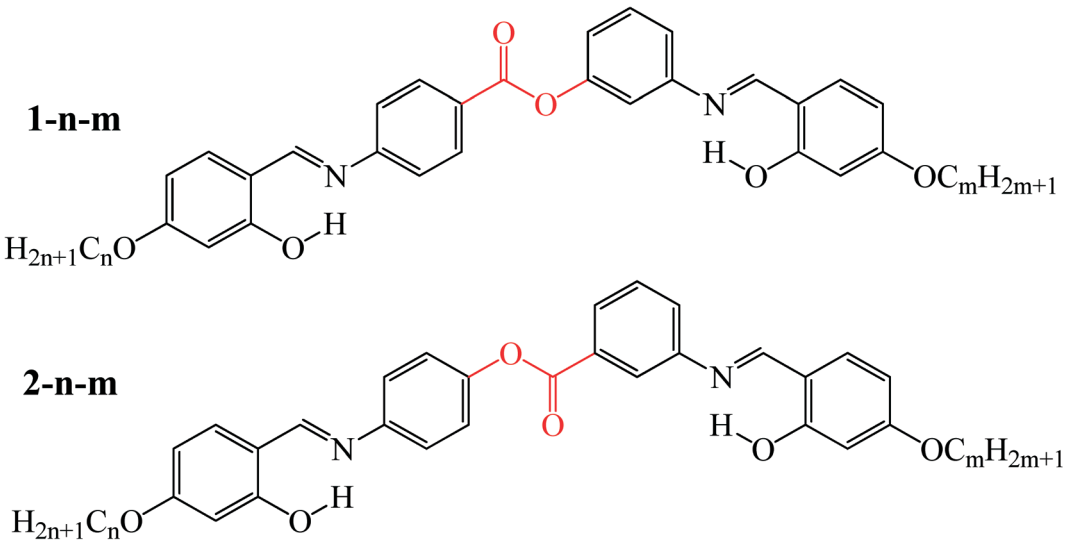

Compound	Phase transition temperatures in °C (enthalpy, entropy)	Mesomorphic range in °C
1-10-11	Cr 104.5 (22.5, 59.5) B_7 110.4 (7.20, 18.7) Iso	6.2
	Cr 86.7 (27.6, 76.7) B_7 108.3 (7.88, 20.6) Iso	21.6
1-12-11	Cr 104.2 (19.2, 51.0) B_7 110.6 (7.77, 20.2) Iso	6.4
	Cr 85.3 (26.2, 73.2) B_7 108.8 (9.08, 23.7) Iso	23.5
1-13-11	Cr 105.6 (30.5, 80.7) B_7 112.4 (14.5, 37,8) Iso	6.8
	Cr 86.9 (44.3, 123.3) B_7 110.0(13.8, 36.2) Iso	23.1
1-14-11	Cr 102.0 (26.8, 71.5) B_7 112.0(12.5, 32.5) Iso	10.0
	Cr 85.6 (43.7, 122.1) B_7 110.4(11.3, 29.4) Iso	24.8
1-15-11	Cr 104.1 (26.8, 72.5) B_7 114.9 (14.9, 38.8) Iso	13.9
	Cr 90.6 (48.3, 135.0) B_7 113.2 (12.9, 33.6) Iso	25.5
1-16-11	Cr 93.6 (17.3, 47.3) B_7 106.9 (7.92, 20.8) Iso	13.3
	Cr 80.8 (25.4, 71.9) B_7 103.9 (4.18, 11.1) Iso	23.1
1-11-15	Cr 103.3 (31.5, 83.9) B_7 114.5 (14.7, 38.0) Iso	11.2
	Cr 90.6 (56.5, 155.6) B_7 113.0 (13.7, 35.6) Iso	22.4
2-10-11	Cr 136.9 (59.2, 144.5) Cr1 147.2 (24.5, 58.3) Iso	—
	Cr 117.3 (43.2, 110.9) B_7 138.0 (16.6, 40.4) Iso	20.7
2-12-11	Cr 134.6 (53.1, 130.5) B_1 139.9 (18.9, 45.8) Iso	5.7
	Cr 114.8 (51.1, 132.1) B_1 138.6 (19.2, 46.7) Iso	24.5
2-14-11	Cr 122.5 (29.9, 75.7) B_1 134.4 (11.0, 27.1) Iso	11.9
	Cr 102.1 (32.3, 86.1) B_1 131.9 (9.06, 22.3) Iso	29.8
2-16-11	Cr 123.0 (32.5, 82.1) B_1 134.1 (11.5, 28.4) Iso	11.1
	Cr 101.3 (32.3, 86.3) B_1 131.0 (10.4, 25.9) Iso	29.7
2-11-12	Cr 133.5 (50.6,124.5) B_1 140.0 (19.3,46.8) Iso	6.5
	Cr 115.7 (49.1,126.5) B_1 138.5 (19.3,47.0) Iso	22.8
2-11-13	Cr 131.7 (57.0,141.0) B_1 138.9 (20.2,49.2) Iso	7.2
	Cr 114.2 (57.7, 149.0) B_1 137.7 (22.2,54.1) Iso	23.5
2-11-15	Cr 128.3 (49.5,123.3) B_1 138.6 (19.5,47.5) Iso	10.3
	Cr 112.6 (50.0,129.6) B_1 137.5(19.9,48.5) Iso	24.9

[a] All compounds exhibited enantiotropic crystal–crystal transitions and are not tabulated.

on an untreated glass plate and coverslip are presented in Fig. 3d and e.

The observed representative optical textures exhibited by compounds of **2-*n*-*m*** homologues are presented in Fig. 4. Upon very slow cooling from the isotropic liquid, compounds of **2-*n*-*m*** (***m*** = 11, ***n*** = 10, 12, 14 and 16; ***m*** = 12, 13 and 15, ***n*** = 11) exhibited a pseudo-broken fan like texture with extinction brushes directed along the polarizer directions. On further cooling low birefringent stripes appeared across the blades of the columnar fan and finally became uniform without any changes in the columnar texture before it crystallizes as shown in Fig. 4. The developable domain-like textures exhibited by the different homologues of the **2-*n*-11** series resemble the textures exhibited by the B1 phase and the

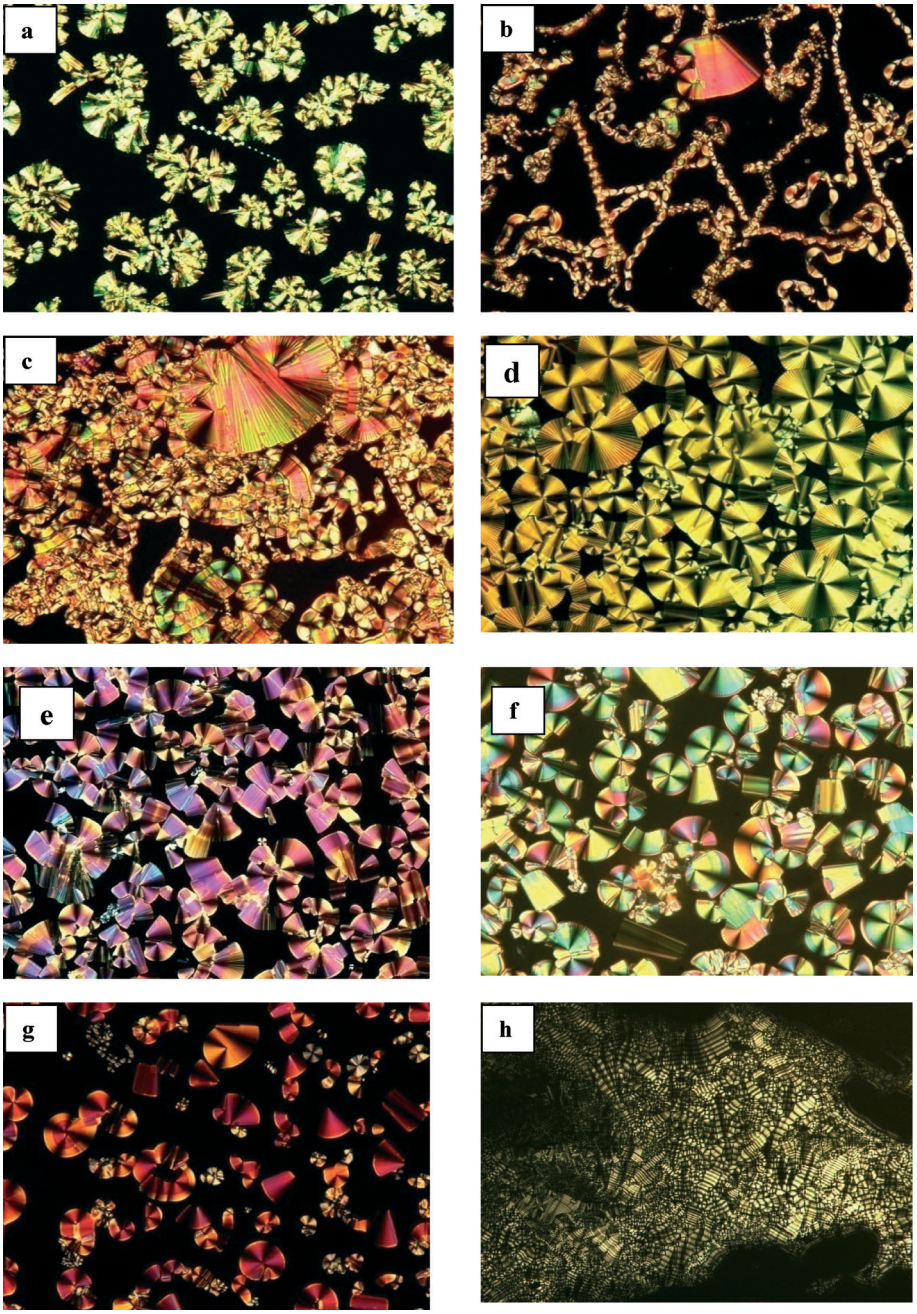

Fig. 3 Typical textures observed in the B_7 phase of a **1-*n*-11** homologue (a) the growth of a dendritic texture with spiral filaments of **1-6-11**; (b) the helical spiral texture formation from the isotropic phase of **1-10-11**; (c) the full growth of the texture shown in b; (d) the **1-12-11** fan-shaped texture in a 5 μm cell at 103 °C; (e) **1-12-11** in a normal glass plate at 108 °C; (f) and (g) the fan-shaped texture of compounds **1-13-11** and **1-14-11**; (h) the optical texture of an uncovered free drop of the B7 phase equally spaced striped pattern of **1-11-15** at 112.5 °C.

optical textures resemble the 2D polarization splay modulated layer undulated smectic phases of the $B7/B1_{RevTilt}$ family.[22,23] On further cooling, the compound exhibited a structured columnar fan like texture.

All the homologues (**1-*n*-*m*** and **2-*n*-*m***) exhibited banana liquid crystalline behaviour over a moderate temperature range of ~20–30 °C in the cooling cycle. The influence of the ester linkage direction is reflected in the clearing transition temperatures. The clearing temperatures of **2-*n*-11** are greater than the **1-*n*-11** homologues by almost 30 °C. The mesomorphic thermal range of **1-*n*-11** and **2-*n*-11** as a function of the number of carbons in the end alkyl chain length is depicted in Fig. S4a and S4b (ESI†). All of the compounds were found to exhibit one mesophase only, exhibiting similar textures. On increasing the length of the end alkoxy chain the mesomorphic range slightly increases from 21 °C (n = 10) to 25 °C (n = 14) and further decreases. A decreasing trend of the melting and clearing transition temperatures with

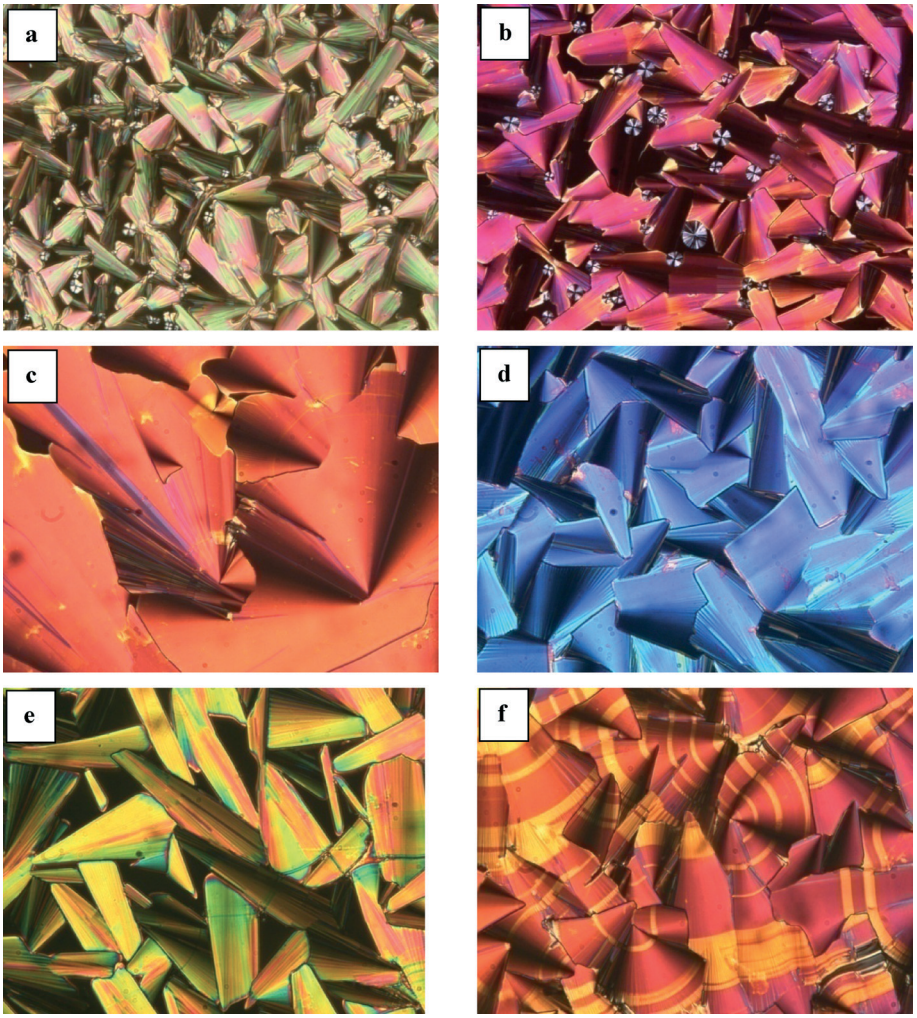

Fig. 4 Typical textures observed of the **2-*n*-11** homologue (a) at 133.3 °C of **2-10-11**, developable domains; (b) **2-12-11** in a normal glass plate; (c) and (d) focal conic B_1 of **2-12-11** in different cell thickness 3.5 and 9 μm respectively; (e) at 130.6 °C of compound **2-14-11**; (f) the fully developed columnar texture of the 2D modulated smectic phases of compound **2-16-11**.

the increasing chain length of the terminal alkoxy chains is observed.

On application of the triangular-wave electrical field of 100 Vpp the switching current response (Ps), varying the frequency from 0.1 Hz, 0.5 Hz and 1.0 Hz, was investigated in the LC phase at 100 °C. A large broad peak was observed up to 0.1 Hz (Fig. S5a–c†), which decreased with an increase in the frequency, and disappeared at a frequency larger than 1.0 Hz (Fig. S5d†). The diminishing broad peak at very low frequencies can be attributed to ionic relaxation. Hence the absence of polarization in the current peak above 1 Hz indicated the absence of switching in this phase.

4. X-ray studies

To confirm the mesophase structures XRD measurements were performed on a few representative compounds **1-10-11**, **1-15-11** and **2-12-11** to get information on the structural aspects, and the diffractograms are displayed in Fig. 5a–c. Fig. 5(a) and (b) shows representative diffractograms (intensity *versus* 2θ profile) in the mesophase at 108 °C and 95 °C for the compounds **1-10-11** and **1-15-11**, respectively. The broad diffuse peak in the wide angle region corresponding to spacing of 4.5 Å confirms the liquid like ordering of the phases. In the small angle region the compound **1-10-11** exhibits four sharp reflections whereas the compound **1-15-11** shows an additional sharp reflection. The indexing carried out for the reflections with incommensurable scattering vectors in the small angle region and they fitted very well (with low χ^2 value) for the tilted columnar phase (Col_{ob}) with the lattice parameters and tilt angle being tabulated in Table 2. The textural patterns described in the earlier section for the **1-*n*-11** series corroborates the X-ray investigations to assign the phase as B7. Such kind of indexing for B7 mesophase to the Col_{ob} phase is well known in the literature.[22,23] The spacing number of the primary peak is smaller than the length of the molecule in both compounds. Perhaps this could be due to the partial overlap of aromatic cores of the antiparallel arranged molecules and interdigitation of the terminal alkyl chains as depicted in the proposed model (Fig. 6).

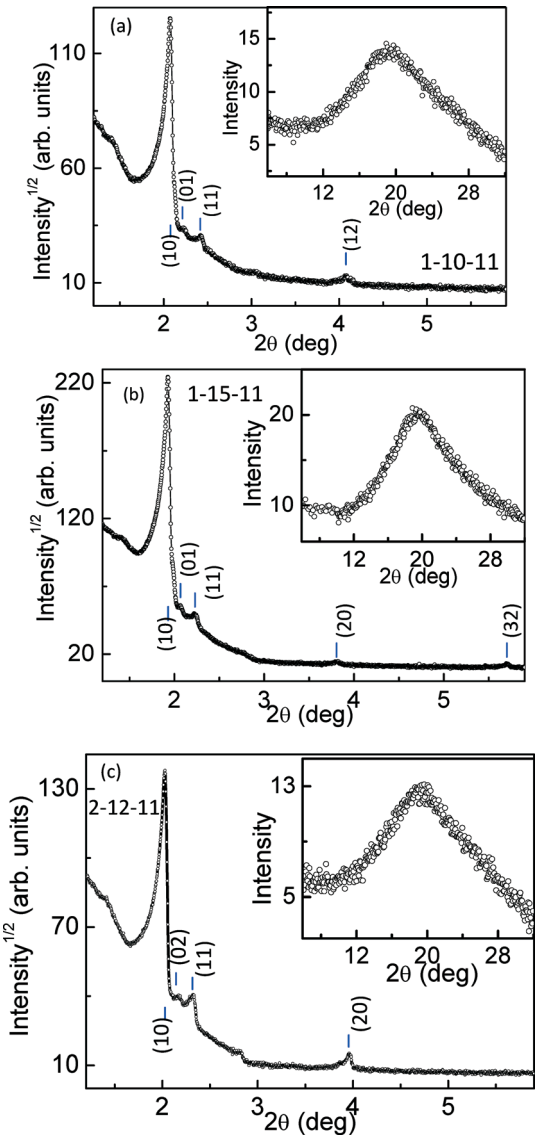

Fig. 5 (a) The X-ray intensity *versus* 2θ profile in the low angle region (main panel) and wide angle (inset) regions for the compound **1-10-11** at T = 108 °C, (b) **1-15-11** at 95 °C and (c) **2-12-11** at 136 °C in the mesophase.

Fig. 5(c) shows representative diffractograms in the mesophase at 136 °C for compound **2-12-11**. With the textural pattern discussed in the earlier section for the **2-*n*-11** series at background the indexing carried out for the sharp low angle peaks fitted very well (with low χ^2 value) for the rectangular lattice with the lattice parameters tabulated in Table 2. Thus the phase exhibited by the **2-*n*-11** series can be indexed to mesophase of the B1 type. Again for this compound the spacing value of the primary peak is smaller than the length of the molecule **2-12-11** obtained from the DFT optimised molecular structure in gaseous phase in its most extended conformation in the gaseous phase (see Fig. 7c) although it is likely that a somewhat more bent conformation is adopted in the condensed phases. Perhaps this could be due to the partial overlap of the aromatic cores of the antiparallel arranged molecules and interdigitation of the terminal alkyl chains.

Table 2 The XRD data of the compounds studied. In all the compounds (**1-10-11**, **1-15-11** and **2-12-11**) studied the columnar axis is taken as the *c*-axis and the *ab* the lattice plane

1-10-11 T = 108 °C		d_{meas} (Å)	d_{calc} (Å)	(hk)
	1	42.54	42.50	(10)
	2	39.93	40.01	(01)
	3	36.57	36.68	(11)
	4	21.68	21.41	(12)
	5	4.54		
a = 45.75 Å; b = 43.06 Å; γ = 68.6°; V = 8952 Å^3				
1-15-11 T = 108 °C		d_{meas} (Å)	d_{calc} (Å)	(hk)
	1	45.48	45.67	(10)
	2	42.15	42.11	(01)
	3	37.97	38.13	(11)
	4	23.11	22.84	(20)
	5	15.46	15.01	(32)
	6	4.54		
a = 48.60 Å; b = 44.81 Å; γ = 70°; V = 9880 Å^3				
T = 95 °C				
	1	45.79	45.91	(10)
	3	42.73	42.73	(01)
	4	39.62	39.61	(11)
	5	23.22	22.96	(20)
	6	15.50	15.52	(32)
	6	4.51		
a = 49.58 Å; b = 46.14 Å; γ = 67.6°; V = 10313 Å^3				
2-12-11 T = 136 °C		d_{meas} (Å)	d_{calc} (Å)	(hk)
	1	43.57	43.60	(10)
	2	41.19	41.22	(02)
	3	38.16	38.52	(11)
	4	22.34	21.80	(20)
	5	4.57		
a = 43.60 Å; b = 82.24 Å; V = 16386 Å^3				

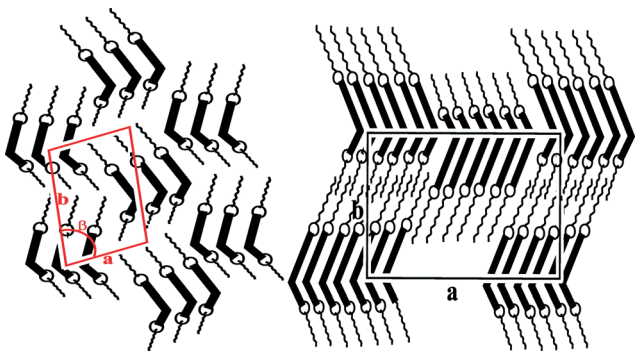

Fig. 6 A proposed model structure for the Col_{ob} (B7) phase and Col_r (B1) phase exhibited four-ring bent-core compounds with unequal arms of aromatic cores.

It is about 7 molecules of **1-10-11** or **1-15-11** compounds and about 12 molecules of **2-12-11** compound organize to form one slice to fit into the column. Based on the XRD and textural studies the mesophase exhibited by the **1-*n*-11** series can be identified as the B7 type and **2-*n*-11** series to the B1 type.

The formation spiral domains and 2D focal conic textures, the multiple peak reflections at low angles, the tilt in the molecular layering and the non-switchable phase structure are indicative of a $B_7/B1_{RevTilted}$ phase structure and suggest

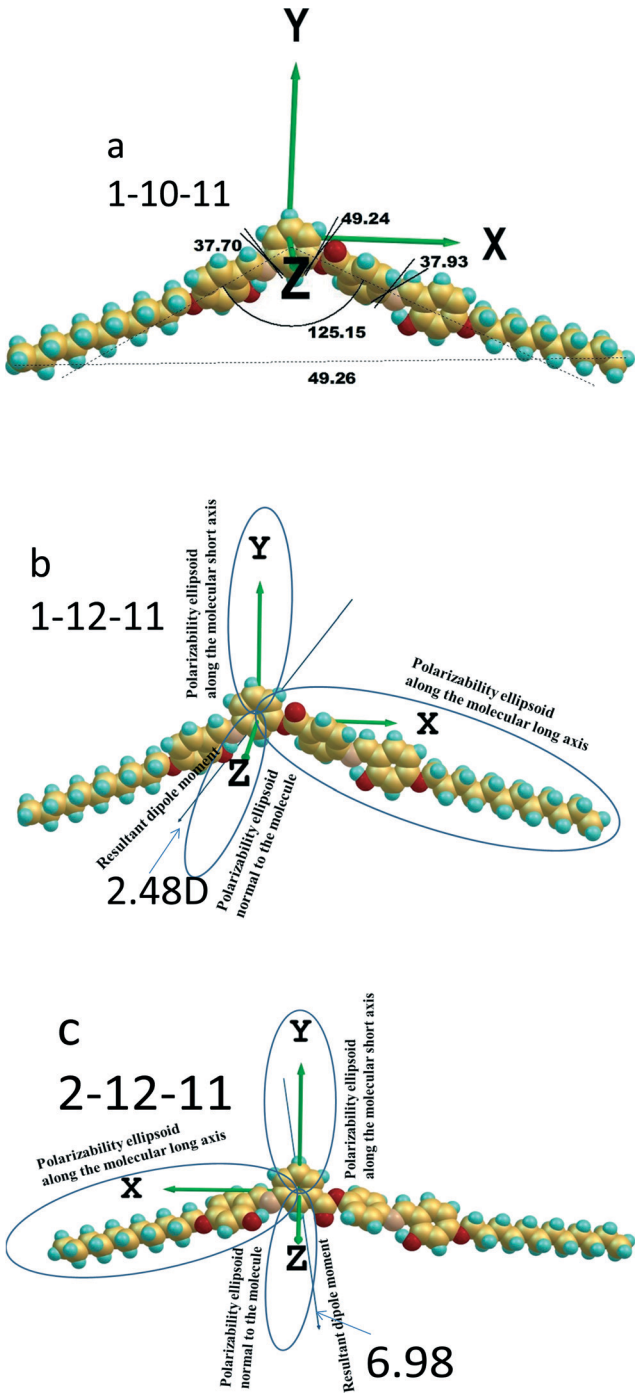

Fig. 7 The DFT calculated minimised energy conformation of the molecular structure (a) in the fully extended all trans conformation of **1-10-11** with a bent angle 125° and dihedral angles (37°, 49°, 37°) showing the twisted molecular structure (b) the polarizability ellipsoid and resultant dipole moment direction of **1-12-11** (c) the polarizability ellipsoid and resultant dipole moment direction of **2-12-11**.

that the phase represents the 2D polarization splay modulated layer undulated molecular structure of the SmCPU family.[11,12] The 2D structure of columnar phases is a result of chiral symmetry breaking, which occurs in these bent-core molecules if they are tilted with respect to the smectic layer normal. The tilt of the molecules is evidenced from the X-ray studies. The strong coupling between the polarization splay and the tilt of the molecules led to 2D modulated phases *viz.*, polarization modulated and layer undulated phases or columnar phases and are evidenced in the optical textures resembling the similar phases reported earlier. Furthermore, contrary to earlier reports[2,3m] on the influence of the core structure in the formation of modulated phases, a decrease in the size of the core structure (4 rings) with increased alkyl chain lengths can also form columnar structures. Therefore it appears that the columnar phase is only stable if a partial overlap of the aromatic cores of the antiparallel arranged molecules at the border between the two columnar blocks is possible.

5. DFT studies

A DFT computational study based on quantum mechanical calculations was performed to obtain the information related to the molecular conformation, bend angle, dipole moment, molecular polarizability and electrostatic potential distribution of the molecules **1-*n*-11** and **2-*n*-11**. Full geometry optimizations have been carried out without imposing any constraints using the Gaussian 09 program package.[32] Spin-restricted DFT calculations were carried out in the framework of the generalized gradient approximation (GGA) using Becke3-Lee-Yang-Parr hybrid functional (B3LYP) exchange–correlation functional and the 6-311G(d,p) basis set.[33,34] The B3LYP functional with the standard basis set 6-311G(d,p) has been used due to its successful application for larger organic molecules, as well as hydrogen bonded systems in the past,[35–37] and bent-core molecules[38–41] recently.

Among the two studied homologous compounds **1-*n*-11** and **2-*n*-11** (Table S1†), the calculated bond lengths are found to be noticeably different. In the central phenyl benzoate core, the dihedral angle is found to be ~49°, between the phenyl carbon and the oxygen atom of the ester linkage. The dihedral angle between the phenyl carbon and nitrogen atom of the imine linkage is found to be ~37°. Furthermore, a significant difference in the bend angles (123 ± 3° and 141°) as well as the dipole moments was found. For example the dipole moment of **1-12-11** is 2.48 D whereas **2-12-11** is 6.98 D (Fig. 7). The major contribution of the dipole moment comes from the Y and Z components of **2-12-11** whereas in the case of **1-12-11**, the major role in the dipole moment is played by the X and Y components. The polarizabilities are crucial for an understanding of the molecular properties in molecular optics and spectroscopy. Electrostatic intermolecular interaction energy is related to this quantity, in particular for systems without a permanent dipole moment.[42] The molecular polarizability component α_{XX} is comparatively larger along the molecular longitudinal *X*-axis (Table S2†) for both molecules (**1-12-11** and **2-12-11**) than the other two directions. However, the asymmetry parameter $\eta = [(\alpha_{YY} - \alpha_{ZZ})/(\alpha_{XX} - \alpha^{iso})]$, which is dependent on the bending angle and polarizability components is found to be distinctly different for the two homologous series (0.4–0.5 and 0.03–0.05) respectively for the

molecules **1-*n*-11** and **2-*n*-11**. The principle components of the polarizability tensor (α_{XX}, α_{YY}, α_{ZZ}) are different but the isotropic polarizability $\alpha^{iso} = (\alpha_{XX} + \alpha_{YY} + \alpha_{ZZ})/3$ is almost same for both homologues. Though the molecular formula and number of electrons of the two studied molecules are the same, the direction of the ester linkage must be the major contributor to the significant differences in the principal components of the polarizabilities and dipole moment, the magnitude of dipole moment, the bend angle and asymmetry parameter. The DFT calculated principal polarizability components (α_{XX}, α_{YY}, α_{ZZ}), the isotropic polarizability component α^{iso}, the polarizability anisotropy $\Delta\alpha = [\alpha_{XX} - (\alpha_{YY} + \alpha_{ZZ})/2]$, and the asymmetry parameter, $\eta = [(\alpha_{YY} - \alpha_{ZZ})/(\alpha_{XX} - \alpha^{iso})]$, which are parameters relative to the molecular polarizability tensor, α, in the Cartesian reference frame are displayed in Fig. 7.

6. UV–Visible and fluorescence studies

The emission properties of organic LCs are currently an active area of research due to their potential applications in opto-electronics. Emissive liquid crystals are intriguing systems for materials research because they couple molecular self-assembly with intrinsic light generation capability. The unsymmetrical bent-core plays an important role in the modification of the electronic characteristics of the molecules. Hence the absorption and emission properties of a representative compound were studied, and the results of the UV–visible absorption and fluorescence spectroscopic properties of **2-12-11** in chloroform (conc. 1.0×10^{-5} M) were studied in solution, to obtain information regarding the absorption and emission maxima and the Stokes shift of fluorescence are presented. The UV–visible spectra in these homologous compounds exhibited strong absorption peaks at ~350 nm with a large molar extinction coefficient (Fig. 8, 3.54 eV for **2-12-11**, ε ~ 264 000 L mol^{-1} cm^{-1} concentration = 10^{-5} M solution in $CHCl_3$). The strong absorption band reflects the π–π* transition of the highly π-conjugated system having the substituted phenyl benzoate unit as the core. **2-12-11** is found to exhibit a large Stokes shift (~180 nm), which reflects the structural relaxation of the excited molecule, and is significantly larger than that reported in push–pull systems exhibiting liquid crystal behaviour[43–47] reflecting changes in the molecular conformation upon excitation. These results are in good agreement with the reported results of molecular J-aggregates[48] in which the excitonic energy is delocalized as a result of the intermolecular coupling within the head-to-tail arrangement of the molecules in the solution.

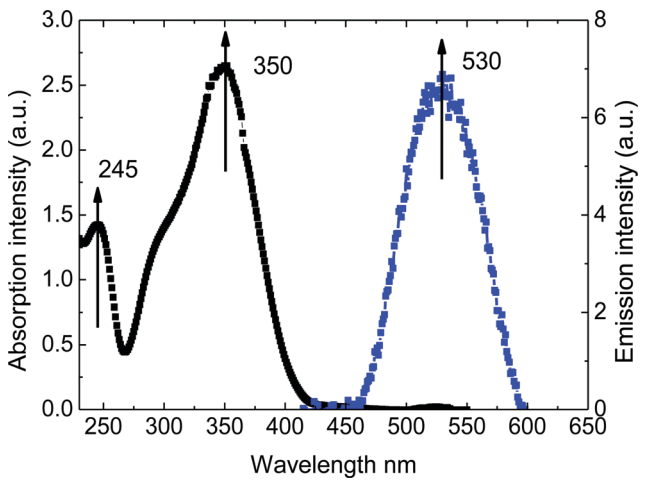

Fig. 8 UV–visible and fluorescent spectra of **2-12-11** in chloroform ($C = 10^{-5}$).

7. Conclusions

Unsymmetrical four-ring bent-core compounds with unequal chain lengths and reversing the ester linkage in the molecule have been designed, successfully synthesized and characterized. It is interesting to note that the 1-series exhibit the B7 phase with an oblique columnar lattice, while the 2-series exhibits a B1 phase family with a rectangular lattice. Bent-core molecules of uneven aromatic–aliphatic moieties are ideal candidates to exhibit 2D polarization splay modulated and layer undulated phases of $B_7/B_{1RevTilted}$ structures. The interaction of molecules within the layers and/or between the layers can lead to layer modulations. The hydroxyl group in the wings of these molecules participate in inter and/or intra-molecular H-bonding which adds to the strength and molecular interactions in the formation of undulated and modulated smectic phases. The influence of the carbonyl direction reflected in a significant change in the magnitude of dipole moment of the molecules which will contribute to the physical properties of these compounds as well as the phase structure.

Acknowledgements

Financial assistance provided by the Department of Atomic Energy, the Department of Science and Technology, the Naval Research Board and University Grants commission India is gratefully acknowledged.

References

1 T. Niori, T. Sekine, J. Watanabe, T. Furukawa and H. Takezoe, *J. Mater. Chem.*, 1996, **6**, 1231.
2 D. R. Link, G. Natale, R. Shao, J. E. Maclennan, N. A. Clark, E. Korblova and D. M. Walba, *Science*, 1997, **278**, 1924.
3 G. Pelzl, S. Diele and W. Weissflog, *Adv. Mater.*, 1999, **11**, 707.
4 R. A. Reddy and C. Tschierske, *J. Mater. Chem.*, 2006, **16**, 907.
5 H. Takezoe and Y. Takanishi, *Jpn. J. Appl. Phys.*, 2006, **45**, 597.
6 C. Tschierske and G. Dantlgraber, *Pramana*, 2003, **61**, 455.
7 M. B. Ros, J. L. Serrano, M. R. de la Fuente and C. L. Folcia, *J. Mater. Chem.*, 2005, **15**, 5093.
8 A. Jakli, C. Bailey and J. Harden, *Thermotropic liquid crystals*, ed. A. Ramamoorthy Springer, The Netherlands, 2007, pp. 59–83.

9 A. Eremin and A. Jakli, *Soft Matter*, 2013, **9**, 615.
10 (*a*) C. Keith, A. Lehmann, U. Baumeister, M. Prehm and C. Tschierske, *Soft Matter*, 2010, **6**, 1704; (*b*) O. Francescangeli, F. Vita, C. Ferrero, T. Dingemans and E. T. Samulski, *Soft Matter*, 2011, **7**, 895; (*c*) O. Francescangeli and E. T. Samulski, *Soft Matter*, 2010, **6**, 2413; (*d*) S. Chakraborty, J. T. Gleeson, A. Jakli and S. Sprunt, *Soft Matter*, 2013, **9**, 1817.
11 (*a*) V. Gortz and J. W. Goodby, *Chem. Commun.*, 2005, 3262; (*b*) V. Gortz, C. Southern, N. W. Roberts, H. F. Gleeson and J. W. Goodby, *Soft Matter*, 2009, **5**, 463; (*c*) G. Pelzl, A. Eremin, S. Diele, H. Kresse and W. Weissflog, *J. Mater. Chem.*, 2002, **12**, 2591; (*d*) W. Weissflog, S. Sokolowski, H. Dehne, B. Das, S. Grande, M. W. Schröder, A. Eremin, S. Diele, G. Pelzl and H. Kresse, *Liq. Cryst.*, 2004, **31**, 923; (*e*) T. Niori, J. Yamamoto and H. Yokoyama, *Mol. Cryst. Liq. Cryst.*, 2004, **409**, 475.
12 R. B. Meyer, *Mol. Cryst. Liq. Cryst.*, 1977, **40**, 33.
13 I. C. Pintre, J. L. Serrano, M. B. Ros, J. Martínez-Perdiguero, I. Alonso, J. Ortega, C. L. Folcia, J. Etxebarria, R. Alicante and B. Villacampa, *J. Mater. Chem.*, 2010, **20**, 2965.
14 D. K. Yoon, Y. Yi, Y. Shen, E. Korblova, D. M. Walba, I. I. Smalyukh and N. A. Clark, *Adv. Mater.*, 2011, **23**, 1962.
15 F. Araoka, G. Sugiyama, K. Ishikawa and H. Takezoe, *Adv. Funct. Mater.*, 2013, **23**, 2701.
16 H. R. Brand, P. E. Cladis and H. Pleiner, *Eur. Biophys. J.*, 1998, **6**, 347.
17 K. Saito, T. Shinhara, T. Nakamoto, S. Kutsumizu, S. Yano and M. Sorai, *Phys. Rev. E: Stat., Nonlinear, Soft Matter Phys.*, 2002, **65**, 031719.
18 (*a*) K. Horiuchi, Y. Yamamura, R. Pełka, M. Sumita, S. Yasuzuka, M. Massalska-Arodz and K. Saito, *J. Phys. Chem. B*, 2010, **114**, 4870; (*b*) C. Tschierske, *J. Mater. Chem.*, 1998, **8**, 1485.
19 Y. Yamaoka, Y. Taniguchi, S. Yasuzuka, Y. Yamamura and K. Saito, *J. Chem. Phys.*, 2011, **135**, 044705.
20 (*a*) F. Hardouin, H. T. Nguyen, M. F. Achard and A. M. Levelut, *J. Phys., Lett.*, 1982, **43**, L-32; (*b*) A. M. Levelut, *J. Phys., Lett.*, 1984, **45**, 603.
21 S. Diele, K. Zierbarth, G. Pelzl, D. Demus and W. Weissflog, *Liq. Cryst.*, 1990, **8**, 211.
22 (*a*) D. A. Coleman, J. Fernsler, N. Chattham, M. Nakata, Y. Takanishi, E. Korblova, D. R. Link, R. F. Shao, W. G. Jang, J. E. Maclennan, O. M. Monval, C. Boyer, W. Weissflog, G. Pelzl, L. C. Chien, D. M. Walba, J. Zasadzinski, J. Watanabe, H. Takezoe and N. A. Clark, *Science*, 2003, **301**, 1204; (*b*) G. Pelzl, M. A. Schroder, U. Dunemann, S. Diele, W. Weissflog, C. Jones, D. Coleman, N. A. Clark, R. Stannarius, J. Li, B. Das and S. Grande, *J. Mater. Chem.*, 2004, **14**, 2492; (*c*) D. A. Coleman, C. D. Jones, M. Nakata, N. A. Clark, D. M. Walba, W. Weissflog, K. Fodor-Csorba, J. Watanabe, V. Novotna and V. Hamplova, *Phys. Rev. E: Stat., Nonlinear, Soft Matter Phys.*, 2008, 77, 021703.
23 (*a*) J. Szydlowska, J. Mieczkowski, J. Matraszek, D. W. Bruce, E. Gorecka, D. Pociecha and D. Guillon, *Phys. Rev. E: Stat. Phys., Plasmas, Fluids, Relat. Interdiscip. Top.*, 2003, **67**, 031702; (*b*) J. Svoboda, V. Novotna, V. Kozmık, M. Glogarova, W. Weissflog, S. Diele and G. Pelzl, *J. Mater. Chem.*, 2003, **13**, 2104; (*c*) C. L. Folcia, J. Etxebarria, J. Ortega and M. B. Ros, *Phys. Rev. E: Stat., Nonlinear, Soft Matter Phys.*, 2005, **72**, 041709; (*d*) N. Vaupotic and M. Copic, *Phys. Rev. E: Stat., Nonlinear, Soft Matter Phys.*, 2005, **72**, 031701; (*e*) C. L. Folcia, I. Alonso, J. Ortega, J. Etxebarria, I. Pintre and M. B. Ros, *Chem. Mater.*, 2006, **18**, 4617; (*f*) N. Vaupotic, M. Cepic, E. Gorecka and D. Pociecha, *Phys. Rev. Lett.*, 2007, **98**, 247802; (*g*) D. Pociecha, N. Vaupotic, E. Gorecka, J. Mieczkowski and K. Gomola, *J. Mater. Chem.*, 2008, **18**, 881; (*h*) E. Gorecka, D. Pociecha, N. Vaupotic, M. Cepic, K. Gomola and J. Mieczkowski, *J. Mater. Chem.*, 2008, **18**, 3044; (*i*) M. Kohout, J. Svoboda, V. Novotna, D. Pociecha, M. Glogarova and E. Gorecka, *J. Mater. Chem.*, 2009, **19**, 3153; (*j*) N. Vaupotic, D. Pociecha, M. Cepic, K. Gomola, J. Mieczkowski and E. Gorecka, *Soft Matter*, 2009, **5**, 2281; (*k*) V. Kozmik, P. Polasek, A. Seidler, M. Kohout, J. Svoboda, V. Novotna, M. Glogarova and D. Pociecha, *J. Mater. Chem.*, 2010, **20**, 7430; (*l*) J. Watanabe, T. Niori, T. Sekine, T. Furukawa and H. Takezoe, *Jpn. J. Appl. Phys.*, 1998, **37**, L139; (*m*) D. Shen, A. Pegenau, S. Diele, I. Wirth and C. Tschierske, *J. Am. Chem. Soc.*, 2000, **122**, 1593.
24 (*a*) V. Kozmık, M. Kuchar, J. Svoboda, V. Novotna, M. Glogarova, U. Baumeister, S. Diele and G. Pelzl, *Liq. Cryst.*, 2005, **32**, 1151; (*b*) V. Kozmık, A. Kovarova, M. Kuchar, J. Svoboda, V. Novotna, M. Glogarova and J. Kroupa, *Liq. Cryst.*, 2006, **33**, 41.
25 (*a*) F. C. Yu and L. J. Yu, *Chem. Mater.*, 2006, **18**, 5410; (*b*) J. H. Wild, K. Bartle, M. O'Neill, S. M. Kelly and R. P. Tuffin, *Liq. Cryst.*, 2006, **33**, 635; (*c*) M. Hird, Y. Raoul, J. W. Goodby and J. Gleeson, *Ferroelectrics*, 2004, **309**, 95; (*d*) K. M. Fergusson and M. Hird, *J. Mater. Chem.*, 2010, **20**, 3069; (*e*) K. M. Fergusson and M. Hird, *Adv. Mater.*, 2007, **19**, 211; (*f*) M. Hird, J. W. Goodby, J. Gough and K. J. Toyne, *J. Mater. Chem.*, 2001, **11**, 2732; (*g*) A. S. Matharu, C. Grover, L. Komitov and G. Anderson, *J. Mater. Chem.*, 2000, **10**, 1303; (*h*) N. Aziz, S. M. Kelly, W. Duffy and M. Goulding, *Liq. Cryst.*, 2008, **35**, 1279; (*i*) W. Weissflog, U. Dunemann, S. F. Tandel, M. G. Tamba, H. Kresse, G. Pelzl, S. Diele, U. Baumeister, A. Eremin, S. Stern and R. Stannarius, *Soft Matter*, 2009, **5**, 1840; (*j*) S. Kang, Y. Saito, N. Watanabe, M. Tokita, Y. Takanishi, H. Takezoe and J. Watanabe, *J. Phys. Chem. B*, 2006, **110**, 5205.
26 (*a*) R. Deb, R. K. Nath, M. K. Paul, N. V. S. Rao, F. Tuluri, Y. Shen, R. Shao, D. Chen, C. Zhu, I. I. Smalyukh and N. A. Clark, *J. Mater. Chem.*, 2010, **20**, 7332; (*b*) D. K. Yoon, R. Deb, D. Chen, E. Korblova, R. Shao, K. Ishikawa, N. V. S. Rao, D. M. Walba, I. I. Smalyukh and N. A. Clark, *Proc. Natl. Acad. Sci. U. S. A.*, 2010, **107**, 21311; (*c*) R. K. Nath, D. D. Sarkar, D. S. S. Rao and N. V. S. Rao, *Liq. Cryst.*, 2012, **39**, 889; (*d*) R. K. Nath, R. Deb, N. Chakraborty, G. Mohiuddin, D. S. S. Rao and N. V. S. Rao, *J. Mater. Chem. C*, 2013, **1**, 663.
27 (*a*) W. Weissflog, G. Naumann, B. Kosata, M. W. Schroder, A. Eremin, S. Diele, H. Kresse, R. Friedemann, S. A. R. Krishnan and G. Pelzl, *J. Mater. Chem.*, 2005, **15**, 4328; (*b*) S. A. R. Krishnan, W. Weissflog, G. Pelzl, S. Diele,

H. Kresse, Z. Vakhoskaya and R. Friedemann, *Phys. Chem. Chem. Phys.*, 2006, **8**, 1170.
28 (*a*) J. W. Emsley, M. J. C. Furby and G. D. Luca, *Liq. Cryst.*, 1996, **21**, 877; (*b*) T. Tsuji, H. Takeuchi, T. Egawa and S. Konaka, *J. Am. Chem. Soc.*, 2001, **123**, 6381; (*c*) G. Cinacchi and G. Prampolini, *J. Phys. Chem. A*, 2005, **109**, 6290.
29 (*a*) K. Kumazawa, M. Nakata, F. Araoka, Y. Takanishi, K. Ishikawa, J. Watanabe and H. Takezoe, *J. Mater. Chem.*, 2004, **14**, 157; (*b*) S. K. Lee, S. Heo, J. G. Lee, K. T. Kang, K. Kumazawa, K. Nishida, Y. Shimbo, Y. Takanishi, J. Watanabe, T. Doi, T. Takahashi and H. Takezoe, *J. Am. Chem. Soc.*, 2005, **127**, 11085.
30 C. Bailey and A. Jakli, *Phys. Rev. Lett.*, 2007, **99**, 207801.
31 S. K. Prasad, D. S. S. Rao, S. Sridevi, C. V. Lobo, B. R. Ratna, J. Naciri and R. Shashidhar, *Phys. Rev. Lett.*, 2009, **102**, 1478021.
32 M. J. Frisch *et al.*, *GAUSSIAN 09 (Revision B.01)*, Gaussian, Inc., Wallingford, CT, 2010.
33 K. Kim and K. D. Jordan, *J. Phys. Chem.*, 1994, **98**, 10089.
34 P. J. Stephens, F. J. Devlin, C. F. Chabalowski and M. J. Frisch, *J. Phys. Chem.*, 1994, **98**, 11623.
35 A. R. Leach, *Molecular modelling – principles and applications*, Pearson Education Limited, Second edition, England, 2001.
36 N. H. March, *Electron Density Theory of Atoms and Molecules*, Academic, London, 1992.
37 E. S. Kryachko and E. V. Ludena, *Energy Density Functional Theory of Many-Electron System*, Kluwer, Dordrecht, 1990.
38 J. Seltmann, A. Marini, B. Mennucci, S. Dey, S. Kumar and M. Lehmann, *Chem. Mater.*, 2011, **23**, 2630.
39 A. R. K. Selvaraj, W. Weissflog and R. Friedemann, *J. Mol. Model.*, 2007, **13**, 907.
40 A. R. K. Selvaraj, W. Weissflog, G. Pelzl, S. Diele, H. Kresse, Z. Vakhovskaya and R. J. Friedemann, *Phys. Chem. Chem. Phys.*, 2006, **8**, 1170.
41 W. Weissflog, G. Naumann, B. Kosata, M. W. Schroeder, A. Eremin, S. Diele, H. Kresse, R. Friedemann, A. R. K. Selvaraj and G. Pelzl, *J. Mater. Chem.*, 2005, **15**, 4328.
42 W. Koch and M. C. Holthausen, *A Chemist's Guide to Density Functional Theory*, Second Edition, Wiley-VCH Verlag GmbH, 2001.
43 H. Gallardo, R. Cristiano, A. Vieira, R. A. W. Neves Filho, R. M. Srivastava and I. H. Bechtold, *Liq. Cryst.*, 2008, **35**, 57.
44 A. Vieira, R. Cristiano, A. J. Bortoluzzi and H. Gallardo, *J. Mol. Struct.*, 2008, **875**, 364.
45 R. M. Srivastava, R. A. W. Neves Filho, R. Schneider, A. Vieira and H. Gallardo, *Liq. Cryst.*, 2008, **35**, 737.
46 R. Cristiano, F. Ely and H. Gallardo, *Liq. Cryst.*, 2005, **32**, 15.
47 A. Vieira, R. Cristiano, F. Ely and H. Gallardo, *Liq. Cryst.*, 2006, **33**, 381.
48 F. Camerel, L. Bonardi, M. Schmutz and R. Ziessel, *J. Am. Chem. Soc.*, 2006, **128**, 4548.